heritage

Article

Preserving Cultural Heritage: Enhancing Limestone Durability with Nano-TiO_2 Coating

Dorina Camelia Ilieș [1], Andrei-Ionuț Apopei [2], Alexandru Ilieș [1], Tudor Caciora [1,*], Berdenov Zharas [3], Nicolaie Hodor [4], Alexandru Turza [5], Thowayeb H. Hassan [6,7], Lucian Barbu-Tudoran [8], Ana Cornelia Pereș [9], Mariana Ratiu [10], Bahodirhon Safarov [11], Bahadur Bilalov [12] and Emil-Traian Gligor [13]

[1] Department of Geography, Tourism and Territorial Planning, Faculty of Geography, Tourism and Sport, University of Oradea, 1 Universitatii Street, 410087 Oradea, Romania; dilies@uoradea.ro (D.C.I.); ilies@uoradea.ro (A.I.)
[2] Department of Geology, Faculty of Geography and Geology, "Alexandru Ioan Cuza" University of Iași, 700505 Iași, Romania; andrei.apopei@uaic.ro
[3] Faculty of Science, L.N. Gumilyov Eurasian National University, 2 Satpayev Street, Nur-Sultan 010008, Kazakhstan; berdenov_zhg_1@enu.kz
[4] Faculty of Geography, "Babes-Bolyai" University, 5-6 Clinicilor Street, 400006 Cluj-Napoca, Romania; nicolaie.hodor@ubbcluj.ro
[5] National Institute for R&D of Isotopic and Molecular Technologies, 67-103 Donat Street, 400293 Cluj-Napoca, Romania; alexandru.turza@itim-cj.ro
[6] Social Studies Department, College of Arts, King Faisal University, Al Ahsa 31982, Saudi Arabia; thassan@kfu.edu.sa
[7] Tourism Studies Department, Faculty of Tourism and Hotel Management, Helwan University, Cairo 12612, Egypt
[8] Electron Microscopy Center "Prof. C. Craciun", Faculty of Biology & Geology, "Babes-Bolyai" University, 5-7 Clinicilor Str., 400006 Cluj-Napoca, Romania; lucian.barbu@itim-cj.ro
[9] Department of Environmental Engineering, Faculty of Environmental Protection, University of Oradea, Magheru Street 26, 410087 Oradea, Romania; peresana@uoradea.ro
[10] Department of Mechanical Engineering and Automotive, University of Oradea, 410087 Oradea, Romania; mratiu@uoradea.ro
[11] Department of Digital Economy, Samarkand Branch of Tashkent State University of Economics, Samarkand 140105, Uzbekistan; safarovb@rambler.ru
[12] Department of Tourism Business, Azerbaijan University of Tourism and Management, Baku 1172, Azerbaijan; b.bilalov@atmu.edu.az
[13] Department of Civil Engineering, Faculty of Construction, Cadastre and Architecture, University of Oradea, 410058 Oradea, Romania; emil.gligor@didactic.uoradea.ro
* Correspondence: tudor.caciora@yahoo.com; Tel.: +40-740941144

Abstract: External and internal microclimatic conditions, biodeterioration, anthropogenic factors, etc, influence the natural stone support for artifacts and built heritage. Based on this fact, the present study explores the effectiveness of nano-TiO_2 in preserving and enhancing the durability of natural stone used in the façades of heritage buildings, focusing on the Markovits-Mathéser House in Oradea Municipality, Romania. The investigation involved treating rock samples (fossiliferous limestone) with 2% and 5% nano-TiO_2 solutions and subjecting them to simulated extreme climatic conditions for the analyzed area in a controlled climatic chamber for six months. The treated samples demonstrated a significantly higher compressive strength than untreated benchmarks. SEM analyses confirmed that nano-TiO_2 formed a protective layer, filling micro-cracks and pores, thereby enhancing the stone's resistance to environmental stressors. The study also found that the nanoparticle coating maintained its integrity under extreme temperature and humidity variations, with only a slight decrease in surface coverage. These findings suggest that nano-TiO_2 coatings significantly improve heritage building materials' mechanical properties and longevity. However, the study highlights the importance of careful application and long-term evaluation to ensure environmental and health safety. Overall, nano-TiO_2 presents a promising solution for the conservation of cultural heritage, offering enhanced durability and protection against climatic and environmental challenges. Further research is recommended to optimize application workflow and formulations for broader and more effective use in heritage conservation.

check for updates

Citation: Ilieș, D.C.; Apopei, A.-I.; Ilieș, A.; Caciora, T.; Zharas, B.; Hodor, N.; Turza, A.; Hassan, T.H.; Barbu-Tudoran, L.; Pereș, A.C.; et al. Preserving Cultural Heritage: Enhancing Limestone Durability with Nano-TiO_2 Coating. *Heritage* **2024**, *7*, 4914–4932. https://doi.org/10.3390/heritage7090232

Academic Editor: Michele Betti

Received: 10 July 2024
Revised: 30 August 2024
Accepted: 5 September 2024
Published: 8 September 2024

Keywords: natural stone; nanoparticles; conservation; nano-TiO_2; built heritage; climatic chamber

1. Introduction

The degradation of the natural stone found in the constitution of heritage buildings or support for indoor or outdoor artifacts occurs due to external and internal climatic conditions (temperature, humidity, various atmospheric pollutants, etc.), various types of damage (including biodeterioration), the anthropogenic factors, etc. These factors come into direct or indirect interaction with the rock, which shows susceptibility to various processes and phenomena conditioned by mineralogical–petrographic composition, structure, texture, porosity, and resistance, ultimately leading to its degradation. Among the factors listed previously, climate is recognized as one of the main factors that induce significant risks for heritage elements [1]. Therefore, the preservation and management of the material cultural heritage (CH) [2–4] must also be seen through the spectrum of climate variability that can accelerate or sometimes diminish the processes of decay of the buildings; therefore, the type of approach should be a climate-smart CH type [5,6]. In the cases of built heritage edifices with no control over the internal microclimatic conditions, the indoor climate is predominantly influenced by the external one.

Nowadays, a significant risk for CH is the urban heat island (UHI) phenomenon, which contributes to its degradation through multiple mechanisms. This phenomenon occurs when urban areas register higher temperatures (Ts) than surrounding rural areas due to human activities and changes to the urban environment [7]. First, UHI intensifies thermal stress on building materials, accelerating their deterioration. Increasing Ts can lead to repeated expansion and contraction of materials, causing cracks, structural integrity loss, and chemical deterioration. Studies show that this effect is particularly pronounced in historic buildings in densely populated areas, where the combined impact of UHI and heat waves can triple cooling energy consumption and increase the average operational T by up to 5 °C [8]. Second, UHI contributes to increased relative humidity (RH) through the contribution of anthropogenic sources that emit water vapor, evaporation and evapotranspiration, and impermeable surfaces, thus favoring biodeterioration. High RH can accelerate the growth of molds and other microorganisms that attack building materials, especially stone and wood materials used in heritage buildings [9]. UHI can also intensify the effects of air pollution on historic buildings by increasing the concentration of pollutants, acidifying surfaces, accelerating the deposition of particles, etc. Atmospheric pollutants, such as N and SO, can combine with moisture and form acids that attack building surfaces, accelerating their decay [10]. Studies indicate that to combat the adverse effects of UHI, it is essential to integrate urban planning strategies that include green infrastructure and appropriate building materials capable of reducing heat absorption and emission [11].

Based on these considerations, the specialized literature proved that using nanomaterials could help eliminate the risks associated with CH degradation as much as possible. Nanomaterials offer advanced conservation solutions, including strengthening, protection against pollutants, and prevention of biological deterioration, ensuring sustainable protection of heritage elements against environmental factors [12–16].

The application of titanium dioxide nanoparticles (nano-TiO_2) represents a promising way to preserve built heritage and heritage objects, considering its ability to protect against deterioration caused by climatic and environmental factors. Munafò et al. [17], Ruffolo et al. [18], and Speziale et al. [19] investigate the effectiveness of organic biocides and nano-TiO_2 in reducing microbial colonization on architectural heritage stone surfaces, providing a practical understanding of the applicability of these treatments in the real world. The UHI phenomenon could lead in the coming years to an increase in the concentration of atmospheric NO_x [20], leading to an acidic environment with stone degradation by intensifying the chemical processes specific to this type of environment [21].

In the specialized literature, numerous studies explore the benefits and possible disadvantages of the use of nano-TiO_2 in the protection and preservation of various types of natural stone from building façades and heritage objects, highlighting its photocatalytic and self-cleaning factors, and protection against UV radiation [22]. Nano-TiO_2 is used to clean, protect, and preserve natural stone, thanks to its photocatalytic properties, which break down organic pollutants and prevent degradation by conferring self-purifying and antimicrobial properties, improving durability and aesthetic appearance [12,23–25].

The benefits of applying TiO_2 on marble surfaces used in building façades include the significant reduction of the penetration of organic substances, the growth of algae and lichens on the surface of the marble, and maintenance of the natural aesthetic appearance of the stone over time [26]. The effectiveness of treatments can vary depending on the marble's physical properties, chemical composition, and porosity under various climatic and environmental conditions [27,28]. Treatments with nano-TiO_2 have been associated with increased weather resistance and decreased dirt build-up, helping maintain granite's structural and aesthetic integrity. These treatments can reduce the need for maintenance and damage to granite monuments and façades in polluted environments in urban areas, extending their lifespan [29]. The study by Pozo-Antonio et al. [30] explores the aesthetic effects of adding nano-TiO_2 to silica-based consolidants for better granite preservation.

On ornamental limestone and sandstone surfaces, the use of TiO_2 brings numerous benefits, including reducing the penetration of pollutants and microorganisms. TiO_2 treatments can improve the resistance of these stones to environmental factors such as acid rain and urban pollution. Recent studies have investigated the use of nano-TiO_2 to protect and preserve limestone and sandstone façades, increasing their durability [31,32].

The nanotechnology-based approach for conserving and restoring historical monument buildings made of natural stone provides solutions by developing targeted treatments specifically designed for these materials. Kanth and Soni [33] explore the benefits of nano-TiO_2 in the preservation of various materials (stone, ceramics, glass, and pigments), namely protection against climatic and environmental factors, biodeterioration, and UV radiation, while preserving the aesthetics of the stone. The paper by La Russa et al. [34] examines the use of nano-TiO_2 coatings for CH protection, focusing on the role of bonding in hydrophobic and self-cleaning efficacy, influencing the long-term performance of preservation materials.

The application of nano-TiO_2 on outdoor heritage monuments with natural stone support demonstrated the effectiveness and impact on historical monuments from various regions and historical periods [35], with the significant mitigation of deterioration caused by climatic and environmental factors improving the aesthetic aspect of stone monuments from Italy, Romania, Greece, or Mexico [36–38]. Nano-TiO_2 coatings on stone artifacts inside buildings help maintain cleanliness and reduce the need for frequent maintenance. This is particularly important for delicate objects where mechanical cleaning could cause damage [39]. The work of Ben Chobba et al. [40] reviews recent advances in the use of metal oxide nanomaterials to preserve stone artifacts. Other studies [41] have shown that the photocatalytic effect of nano-TiO_2 plays a crucial role in degrading organic pollutants and inhibiting the growth of microorganisms on treated surfaces, thus enhancing the self-cleaning properties and durability of heritage stone materials exposed to outdoor environments.

In addition to the numerous advantages that the application of nano-TiO_2 has, some studies in the field also indicate its shortcomings. Applying this type of solution can induce significant changes in the physical and chemical properties of stone surfaces, including increased erosion and corrosion resistance, reduced pollutant adhesion, microparticles, and limiting the growth and development of microorganisms [42–44]. The application of nano-TiO_2 can have effects on the aesthetic appearance of stone surfaces, including their gloss and color. According to studies by Pinna et al. [45], Smith et al. [46], and Liu et al. [47], nano-TiO_2 coatings can sometimes produce a slight bleaching effect on the stone, which may or may not be desirable in the context of conservation. Using nano-TiO_2 also raises concerns about the impact on the environment and human health. According to the studies of Keller et al. [48], Li et al. [49], Cho et al. [50], Gomez-Villalb et al. [12], and Ben Chobba et al. [40], the release of TiO_2 nanoparticles into the environment can negatively affect human health (through inhalation of nanoparticles) as well as the environment.

Based on the previously indicated, the objective of the present study is to evaluate the use of nano-TiO_2 in the conservation of the built heritage of an urban area (Oradea Municipality, Romania), where the external pavement is made of natural stone, and the control of internal microclimatic conditions is limited; the influence of external factors is in this case significant. The analyses were carried out in the context of the phenomenon of UHI in which the object of study is located, considering the potential expansion of this phenomenon against the background of the growth of the city, the use of construction materials, the decline of green spaces, and the upward trend of T in recent years [49–51]. The study is particularly relevant for Oradea, where a significant built CH is mostly paved with natural stone (mainly limestone). In this context, the research can serve as a starting model of best practices for the conservation of these structures. The study's specific objective is to determine whether limestone suits the nano-TiO_2 application. The efficiency of nanomaterials has been explored, given their ability to protect against damage caused by variability in climate and environmental factors. This evaluation was conducted by simulating extreme climatic conditions for the Romania and Oradea area in the climate chamber (CC).

Thus, our study aims to demonstrate the potential of nano-TiO_2 in protecting the natural stone used in Oradea's built heritage and provide a reference framework for other cities with similar conditions. Although there are numerous studies on the use of nano-TiO_2 in various applications, the present research is distinguished by the fact that it explores a relatively new field, namely the application of this solution on fossiliferous limestone used in heritage buildings. Thus, our study provides new insights by testing the efficiency of nano-TiO_2 under simulated extreme climatic conditions, relevant to the urban environment subject to the UHI phenomenon. This approach not only expands current knowledge on the protection of heritage materials, but also highlights the potential of nano-TiO_2 in preserving this specific type of stone in the face of climatic and environmental stressors.

2. Materials and Methods

The present case study is represented by the Markovits-Mathéser House, located in the historical center of the Municipality of Oradea, Romania. Due to its central location and the limited knowledge about its construction history, many tourists and residents often overlook and fail to discover it, even though the house is steeped in history and architectural beauty. It was built in the Secession style in 1911, on two levels and with a triangular plan, positioned at the intersection of Libertatii Street and Aurel Lazar Street [52,53] (Figure 1). As is the case with several heritage buildings in the Municipality of Oradea, part of the façade of the Markovits-Mathéser House is covered with fossiliferous limestone up to a height of 1.5 m. Thus, 14 rock samples from the main façade were considered for future analyses, evenly distributed to cover the entire façade (Figure 2). It should be mentioned that the collection of samples was non-invasive, the collected samples being part of larger fragments detached from the plinth of the building in the type of renovation works that took place between 2023 and 2024. The collected samples were subjected to a mechanical cleaning process to remove impurities and contaminants from the surface. Afterward, they were washed with distilled water and dried at room temperature for 24 h to ensure optimal adhesion of the nano-TiO_2 during the treatment.

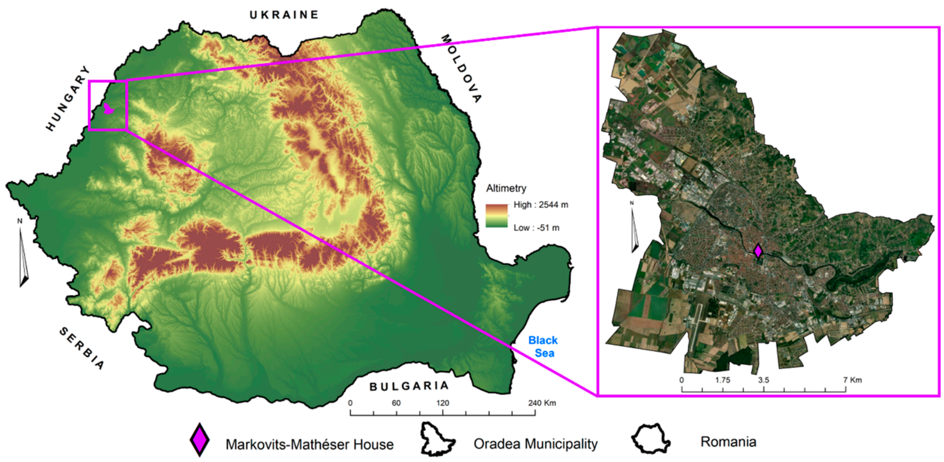

Figure 1. The location of Markovits-Mathéser House at the level of Romania and Bihor County.

Figure 2. Markovits-Mathéser House after renovation and the places where the 14 samples of fossiliferous limestone were collected.

The 14 selected samples followed a detailed workflow, which included several essential steps for determining the mineralogical and petrographic characteristics of the bedrock and evaluating the physical and chemical properties, such as Transmitted Light Polarized Microscopy (TLPM) and Raman Spectra (RS) (Figure 3). These methods allowed the identification of the mineral phases present and the determination of the crystal structure. In the next step, nano-TiO_2 was applied to the surface of all the samples, using specific deposition methods to increase the strength of the material. All samples were then subjected to compression tests (CTs) and Scanning Electron Microscope (SEM) analyses to identify their structural characteristics. The samples were then introduced into the CC and subjected to a controlled climate for a period of six months. Climatic parameters such as T and RH were varied to simulate the extreme environmental conditions to which the materials could be exposed in reality in Oradea Municipality due to UHI. This stage aimed to evaluate the effectiveness of interventions with nano-TiO_2 under rigorous testing conditions, following the hypothesis that UHI has the potential to intensify its action in the future [54,55]. In order to evaluate the effect of nano-TiO_2 on fossiliferous limestone, the standard samples and those introduced in CC were comparatively analyzed using SEM, the degree of nano-TiO_2 coverage (TiO_2-CA), and X-ray Powder Diffraction (XRPD). These analyses aimed to identify the potential differences between the two types of samples in order to draw a conclusion on the applicability of nano-TiO_2 on such fragile samples. At the same time, all samples were analyzed in terms of weight and volume before and after nano-TiO_2 application, respectively, before and after exposure in CC.

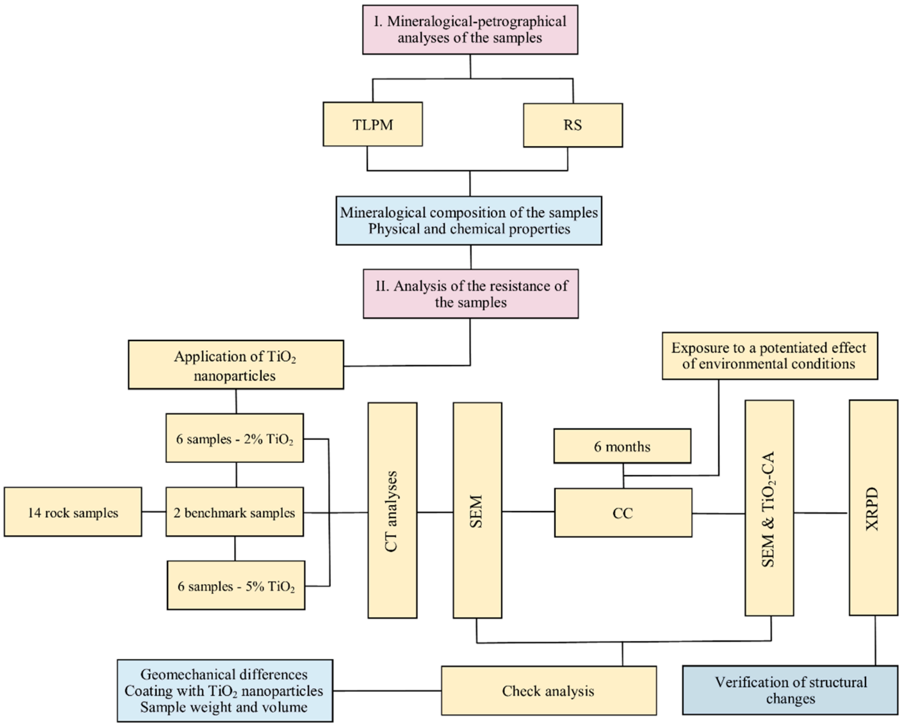

Figure 3. The methodology for implementing the techniques and methods of sample analysis to obtain the results.

All these interventions were aimed at testing a methodology to enhance the durability of materials for future applications and, ultimately, the preservation of CH built with natural stone in the Municipality of Oradea.

2.1. Mineralogical and Petrographical Analyses

Four methods were implemented for the petrographic and mineralogical analysis of the rock samples. These methods determined the mineralogical composition and physical properties of the rock to provide a superior knowledge of the material from which the CH building is made.

Thus, to identify the minerals that make up the rock, TLPM (BX51 Olympus, Tokyo, Japan) equipped with UMPlanFl objectives (5×, 10×, and 20×) was used. A stitch procedure was followed on the entire thin section. TLPM helps identify the different minerals present in the rock sample. Specific minerals can be accurately identified by analyzing the optical properties such as birefringence, pleochroism, and interference colors. TPLM also allows for detailed observation of the rock's texture, including the size, shape, and arrangement of grains and minerals. At the same time, the technique provides insights into microstructural features such as grain boundaries, inclusion patterns, and crystallographic orientations. The comprehensive, high-resolution images obtained through the stitching procedure are valuable for documentation, reporting, and further analysis [56].

A complementary technique to the one previously indicated is the RS, which aims to identify the minerals that make up the rock (it has better accuracy than other techniques), the chemical composition (it can detect the presence of specific molecular bonds and functional groups, helping to determine the chemical make-up of the rock), organic components (it can detect organic compounds within rock samples, which is helpful in studying sedimentary rocks and fossil-containing rocks), mapping, and imaging [57]. The results of this technique were obtained at room T with a Raman Spectrograph Horiba Jobin-Yvon RPA-HE 532 (Horiba Ltd., Kyoto, Japan) with a multichannel air-cooled (−70 °C) CCD detector, using a Nd-Yag laser 532 nm (Horiba Ltd., Kyoto, Japan) excitation source and a nominal power of 100 mW. Spectra were obtained in the spectral range between 210 and

3400 cm^{-1} with a spectral resolution of 3 cm^{-1}. The RS system includes a superhead fiber optic Raman probe for non-contact measurements with a 50× LWD Olympus objective, NA = 0.50, WD = 10.6 mm, and FIB50/10M optical fiber (Newport Corporation, Irvine, CA, USA). The laser spot diameter on the sample surface was approximately 2–3 µm (the minimum theoretical spot diameter is 1.3 µm). Sulfur and cyclohexane were used for the calibration. Data acquisition was performed at a 1–53.6 mW laser power on the sample's surface. Furthermore, the laser power was gradually increased by 1% until any photochemical degradation was observed. Spectra manipulations include essential data treatment, such as smoothing adjustments and peak fitting.

The determination of the geomechanical properties of the stone was made using specific test methods provided in the European and Romanian standards in force regarding various types of rocks, but also taking into account other current research in the field, such as that presented in Búrdalo-Salcedo et al. [58]. In this case, the water absorption test regarding stones covered with a hydrophilic protective layer. The influence of the application method and the number of protective applications on the effectiveness of the treatments is presented in Otero et al. [59].

2.2. Analysis of the Resistance of the Samples

For this case study, a nano-TiO_2 with a size distribution in the 10–30 nm range was selected. The solutions of nano-TiO_2 in concentrations of 2% and 5% were prepared using 0.5 g nano-TiO_2 with 25 mL distilled water (Group A samples) and 1.25 g nano TiO_2 with 25 mL distilled water (Group B samples). These solutions were then applied in the laboratory to rock samples from categories A and B, respectively. The standardized method of applying the solutions was carried out with a brush, ensuring uniformity of treatment. This method involves manual application of the solution with a brush, allowing precise control over the amount of material applied and ensuring adequate coverage of porous surfaces and micro-cracks. Through this technique, nano-TiO_2 forms a homogeneous protective layer, able to fill the interstices and increase the mechanical resistance and durability of the stone in the face of climatic and environmental factors.

To test the hypothesis that materials impregnated with nano-TiO_2 have a higher resistance, a CT was performed on group A and B materials and benchmark samples. The samples for the compression test were prepared by cutting into regular cubes of 50 mm per the UNE standard EN 1926:2007 [60]. Due to the impossibility of taking a sufficient amount of material, which would allow the processing of the samples to the desired size, only five samples were prepared. Three of the five samples were represented by benchmark samples, and two after coating with nanoparticles, in a concentration of 2% nano-TiO_2 and 5% nano-TiO_2, respectively. We mention that the material's structure did not allow the identification of any planes of anisotropy. The determination of the compressive strength was carried out on a 2012 Controls Pilot 4 automatic testing machine, model 50-C5642 (Controls Group, Milan, Italy), which had a maximum compressive capacity of 2000 kN, used for CT of various types of construction materials. Within the device, the precise test parameters were set, namely the dimensions, area, and mass of the samples, including the loading rate, and then the tests were carried out. The loading of the samples was applied continuously, with a constant pressing speed of 0.5 MPa/s.

After applying the solution with nano-TiO_2, all the samples (those with the applied solution and the reference ones) were introduced into the CC. The stability was evaluated using the Memmert Humidity chamber HCP105 (Memmert GmbH + Co., Schwabach, Germany), which is equipped with a controller for RH (1% accuracy of rh) and T (0.1 °C accuracy of T). All the samples were analyzed before their exposure in the CC and upon their exposure for six months at a constant T and RH. The values of the indicators were established following the analysis of T and RH values in the Municipality of Oradea in the period 2011–2024, based on the data acquired from the Oradea Meteorological Station. Thus, Figure 4 shows the values of the two parameters, which recorded multi-year averages of 10.2 °C and 70.5%. Regarding T, the maximum values recorded were 38.8 °C, and the minimum values were −18.9 °C; for RH, the maximum was 100%, and the minimum was 12%.

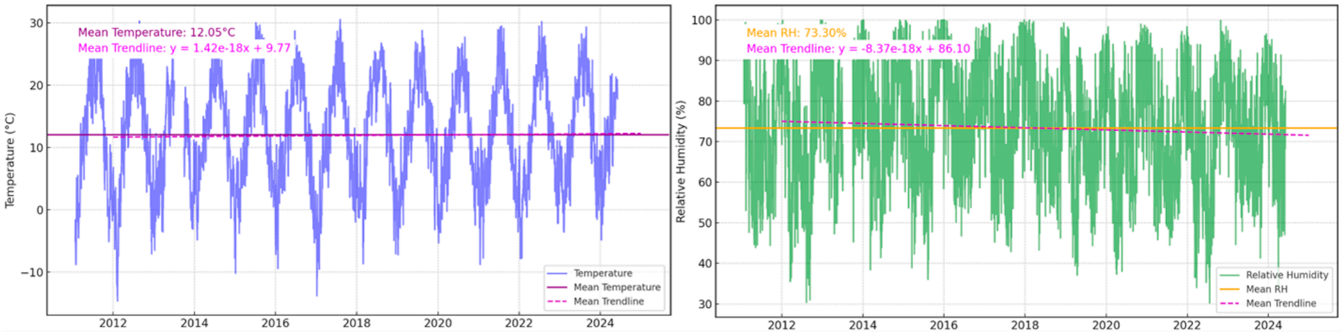

Figure 4. The variation of T and RH values in 2011–2024 in the Municipality of Oradea, Romania. Values based on the parameters to which the samples were subjected in the CC were established.

To establish the values to which the rocks were subjected in CC, it was assumed that they are mainly affected by weathering (the more-or-less sudden change in T and RH) and extreme values. At the same time, based on the trend of increasing T and decreasing RH that can be seen in Figure 4, it was decided to simulate a warmer and drier environment than at present [61] to identify if it can induce damage to the rock and if nano-TiO_2 can slow down or eliminate this risk. In the case of T, the samples were exposed to maximum values of 40.8 °C (+2 °C compared to the maximum from the period 2011–2024) and minimum values of −20.9 °C (−2 °C compared to the minimum from the period 2011–2024). The set values varied more-or-less suddenly, the average for the entire six-month period being 11.2 °C (+1 °C compared to the multi-year average recorded in Oradea during 2011–2024). The Clausius–Clapeyron principle indicates that the capacity of air to retain water vapor increases exponentially with T. On average, for each additional degree Celsius, RH decreases by approximately 5% if the absolute water vapor content remains constant [62]; RH was set to vary significantly between a minimum of 60.5% and a maximum of 80.5% (±10% compared to the multi-year average of RH in Oradea). At the same time, sudden variations of RH were considered, which would follow the trend of extreme situations identified in Oradea in the period 2011–2024. Specifically, the experimental cycles involved exposure of rock samples to low T and high RH for short periods of time (2–3 h), followed by abrupt transitions to high T and low RH for similar durations. In addition to these short-term variations, long-term variation cycles with exposure durations between 2 and 3 days were also implemented, maintaining similar climate characteristics within the CC. These cycles were systematically repeated during the six months of testing in order to evaluate the resistance of nano-TiO_2 to climatic fluctuations of variable intensity and to determine their effectiveness in reducing the impact of weathering and degradation of rocks in urban environments. Repetition of these simulated exposures aims to provide detailed insight into the protective potential of nano-TiO_2 under enhanced climate conditions. In these experiments, we wanted a deeper understanding of the behavior of rocks in boosted climate conditions and the identification of effective conservation solutions using nano-TiO_2.

Before introducing the samples into the CC to carry out the simulations, but also after the completion of the climatic cycle, the rock samples were analyzed with the environmental electron microscope to obtain detailed SEM images to indicate how the surfaces were covered with nano-TiO_2, as well as whether or not they have withstood the boosted climate parameters of CC. For this, the Phenom ProX scanning electron microscope was used, which is particularly useful in studying nanomaterials and structural changes at the micro and nano levels.

The SEM images thus acquired were processed to determine TiO_2—CA before introducing the samples into the CC and after the climatic cycle. This analysis aimed to highlight whether nano-TiO_2 resists the weather and extreme climate in order to conclude its effectiveness. The SEM images were imported into the ImageJ software (v. 1.54j), where their processing was based on contrast and shape. To enhance the differentiation between nanoparticles and constituent minerals, the image contrast was adjusted using dedicated features; the optimal values were established empirically to clearly highlight the nano-TiO_2. The grayscale images were binarized to create a black-and-white image using the optimal contrast threshold. Threshold values were manually adjusted for each image to clarify the separation between nanoparticles (white) and constituent minerals (black). To remove noise and small particles that do not represent nano-TiO_2, the median filter with a radius of 2 pixels was used.

The surfaces covered with nano-TiO_2 were calculated using the particle analysis function. Analysis parameters were set to include particles between 0.5 μm^2 and 50 μm^2 in size and to exclude image edges. Thus, the total percentage of coverage with nano-TiO_2 was calculated based on the formula:

$$S_{TiO_2} = \left(\frac{\sum_{i=1}^{n} A_{TiO_2,i}}{A_t} \right) \times 100 \quad (1)$$

where S_{TiO2} represents the total surface covered with nano-TiO_2, $\sum_{i=1}^{n} A_{TiO_2,i}$ is the sum of the surfaces of the identified nano-TiO_2, A_t is the total surface of the image, and n is the total number of identified particles.

The coverage percentage was determined as the ratio of the total area covered by nano-TiO_2 to the total image area. The software automatically calculated this ratio and saved it in the result table generated by ImageJ.

Finally, XRPD was used to extract valuable structural information regarding the mineralogical composition of the studied samples before and after their CC exposure. This analysis highlights the possible changes in the mineralogical structure suffered by the samples treated with nano-TiO_2 after exposure to the CC conditions. Diffraction data were collected with a Bruker D8 Advance diffractometer (Bruker Corporation, Billerica, MA, USA), operated with the X-ray tube at 40 kV and 40 mA. The diffractometer is equipped with a LYNXEYE detector (Bruker Corporation, Billerica, MA, USA), and a Ge (1 1 1) monochromator was used in order to obtain only the CuKα1 radiation. Among other things, XRPD can accurately reproduce the mineralogical composition and generate semi-quantitative phase analysis, detailed crystallographic information, detection of amorphous content, identification of minor and trace phases, the study of phase transitions and stability, analysis of texture and preferred orientation, grain size and microstrain measurement, detection of polymorphs, correlation with geochemical data, accurate petrographic classification, and non-destructive analysis [63].

3. Results

3.1. Mineralogical–Petrographical Analyses

Thin sections exhibit a biosparite texture, characterized by sparse fossil fragments within a sparite matrix. The sample originates from a carbonate-dominated sedimentary environment, suggesting a depositional history influenced by biological processes and subsequent mineral precipitation. The dominant component observed in this thin section is a bioclastic aggregate consisting of fragmented skeletal remains of marine organisms. While the fossil fragments are not abundant, they are still present and show varying degrees of preservation, ranging from well-preserved to partially dissolved. The most common fossils present include fragments of rotaliids, miliolids, gastropods, and algae, indicating a modest assemblage of marine organisms (Figure 5).

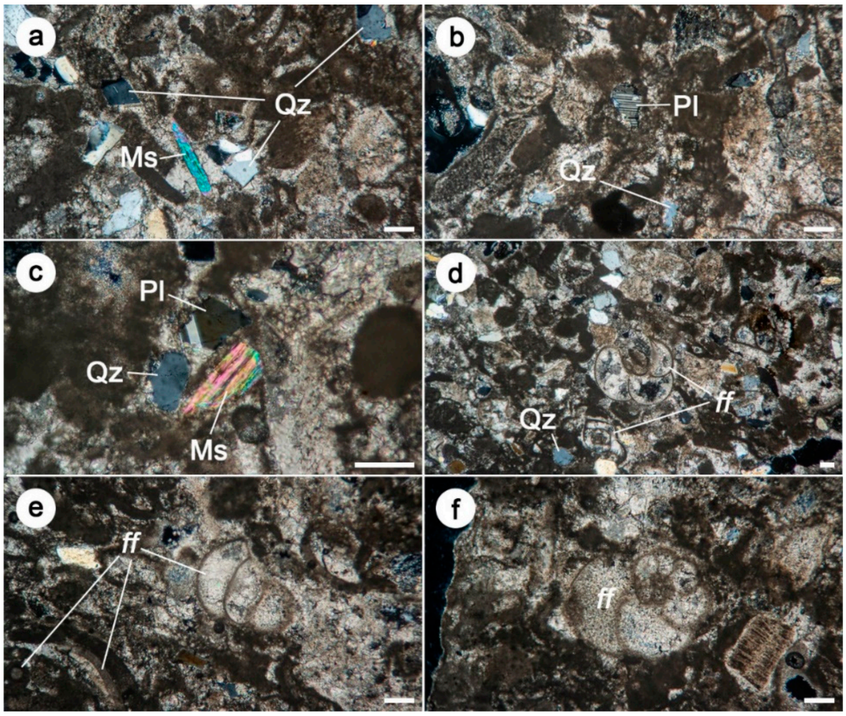

Figure 5. Photomicrographs of thin-sectioned biosparite under crossed polarizers (**a**–**f**). Mineral abbreviation: Qz—Quartz; Ms—Muscovite; Pl—Plagioclase; ff—fossil fragment(s). Scale bars on the photomicrographs are 100 µm.

The matrix of this thin biosparite section is predominantly sparite and composed of fine-to-medium crystalline carbonate minerals. The mineralogy of the sample is completed by anhedral-subhedral quartz crystals, muscovite, and very rare plagioclase feldspar. The carbonate was identified as calcite using RS. The RS of calcite has the characteristic Raman peak located at 1087 cm^{-1} (Figure 6), which is attributed to the ν_1 symmetric stretching vibration of the CO_3 group [22]. The sparite matrix forms a framework that encases and supports the bioclastic fragments. It displays a crystalline texture, with interlocking carbonate crystals of varying sizes, providing a solid framework for the fossils. Within the sparite matrix, the bioclasts are dispersed irregularly throughout the thin section. These bioclasts exhibit a range of sizes, shapes, and orientations. Some may appear angular, indicating minimal transport or alteration, while others may show signs of rounding and abrasion, suggesting reworking and transportation during deposition.

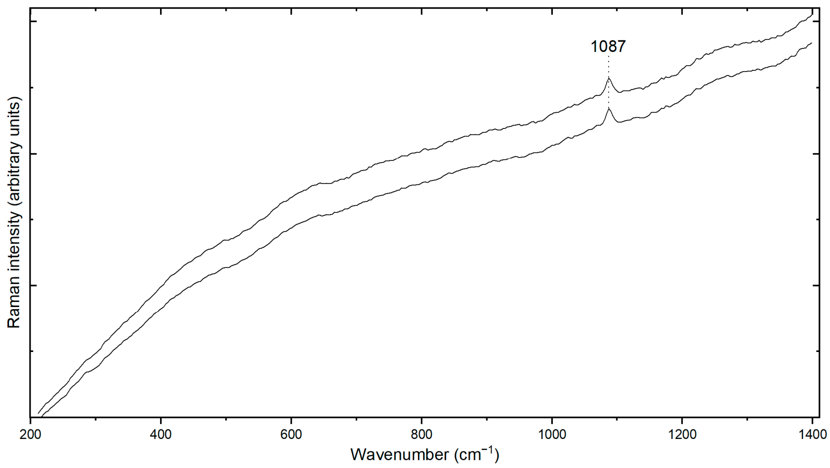

Figure 6. The RS of calcite with the characteristic Raman peak is located at 1087 cm^{-1}. The spectra show high fluorescence due to the laser wavelength of the Raman spectrometer (i.e., 532 nm).

In addition to the bioclasts, small amounts of micritic material are observed within the sparite matrix. These micritic particles likely represent a combination of fine-grained carbonate mud and precipitated carbonate particles. They appear as microcrystalline material interspersed among the broken crystals. Overall, the biosparite thin section represents a carbonate-dominated sedimentary rock characterized by a biosparite texture.

In conclusion, the biosparite thin section, with its sparite matrix and bioclastic fragments, illustrates a carbonate-dominated sedimentary rock formed through biological activity and mineral precipitation in a marine environment.

3.2. Analysis of the Resistance of the Samples

After applying the nano-TiO_2 solutions, the weight of each sample was carefully measured, and a generalized increase in weight was recorded. Data analysis revealed that after application, the weight of each sample increased, indicating the added amount of nano-TiO_2, which varied between 0.04 and 0.13 g (Table 1), depending on the sample and the concentration of the solution used. These data provided details on the amount of nano-TiO_2 involved in the process, thus providing important information for evaluating the impact of nano-TiO_2 solutions on the tested samples.

Table 1. The size and weight of the rock samples before and after the application of nano-TiO_2.

Sample Group	Sample Code	Initial Weight (g)	Quantity of Nano-TiO_2 Applied	Final Weight (g)	Quantity of Nano-TiO_2 Retained (g)
Group A	A1	5.42	2% nano-TiO_2	5.47	0.05
	A2	5.47		5.54	0.07
	A3	4.88		4.93	0.05
	A4	4.39		4.46	0.07
	A5	4.48		4.53	0.05
	A6	5.57		5.62	0.05
Group B	B1	4.78	5% nano-TiO_2	4.85	0.07
	B2	4.84		4.97	0.13
	B3	5.54		5.59	0.05
	B4	5.91		5.97	0.06
	B5	4.19		4.24	0.05
	B6	4.16		4.25	0.09
Benchmark samples	R1	3.31	0% nano-TiO_2	-	-
	R2	4.67		-	-

Regarding CT, the first two reference samples yielded compressive forces of 23.9 kN and 23.5 kN, corresponding to 9.55 MPa and 9.36 MPa compressive strengths. The third standard sample yielded at 12 kN, having a strength of 6.38 MPa, approximately one-third of the values of the other standard samples. Sample 4, coated with 2% nano-TiO_2, yielded 36.4 kN, equivalent to a compressive strength of 14.57 MPa. Sample 5, covered with 5% nano-TiO_2, yielded 49 kN, corresponding to a strength of 19.59 MPa (Figure 7).

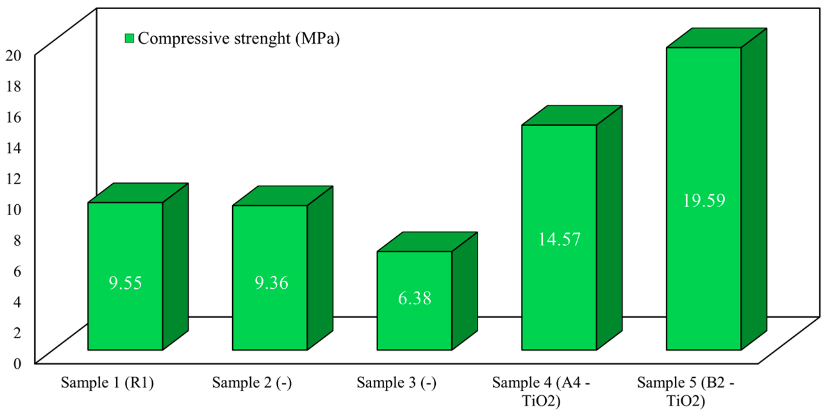

Figure 7. The results obtained for the compression test for the five analyzed rock samples.

The CT results reveal significant differences between the reference samples and those treated with nano-TiO_2, suggesting a positive impact of nanoparticles on the compressive strength of rocks. The samples treated with nano-TiO_2 demonstrated considerably higher compressive strength than the reference ones, with the sample coated with 2% nano-TiO_2 showing strength almost 50% higher (14.57 MPa) and the sample coated with 5% nano-TiO_2 showing strength two times higher (19.59 MPa) compared to the maximum values of the reference samples. The natural variability in the base material is evident, but even the strongest reference sample (9.55 MPa) is well below the strength of the nano-TiO_2-treated samples.

Compared to other studies, the values obtained for CT in this research are lower. Martínez-García et al. [64] reported that 38.5% of uncoated dolostone specimens resisted compressive forces of 200 kN (80 MPa), with strengths increasing with nanoparticle coating of higher concentrations. Dorobat et al. [65] measured average compressive strengths for limestone and crystalline shale of 35 MPa and 43 MPa (parallel to the plane of anisotropy) and 55.4 MPa (perpendicular to the plane of anisotropy) in the dry state, 29 MPa, 33.6 MPa, and 44 MPa, respectively, after 15 freeze–thaw cycles.

The findings demonstrate a significant reduction in the compressive strength of rocks subjected to freeze–thaw cycles. Nevertheless, the application of protective coatings enhances the mechanical strength of the rocks, even under prolonged and severe climatic conditions. This observation accounts for the lower compressive strength values recorded for the fossiliferous limestone specimens evaluated in this study, considering their geological characteristics and historical context. Specifically, these rocks were sourced from slabs at the base of buildings constructed in the 1910s, which have been exposed to environmental weathering for over a century as part of extensive exterior restoration efforts. Based on this last idea, we can say that interventions with nano-TiO_2 are all the more important for the current study, considering the age and the need to preserve the rock.

The analyses aimed at the morphological aspects of the surface of the analyzed fossiliferous limestone; the SEM images show that nano-TiO_2 are capable of uniformizing the surfaces (Figure 8), filling the micro-cracks, interstices, and pores on the surface of the stone, forming a protective layer that can contribute to increasing rock resistance and reducing the impact of climatic and environmental factors [66]. The back-scattered electron images reveal that the particle sizes of nano-TiO_2 range from 0.3 to 0.5 μm, suggesting a consistent and even distribution of sizes. The uniform particle size remains constant regardless of the concentration of nano-TiO_2 or the conditions in the CC. The analyses show that the homogeneity of the coating varies with the concentration of the solution and the storage conditions in the CC. The SEM images provide a visual comparison of the coating's consistency and uniformity before and after exposure to the controlled environment of the CC (Figure 8).

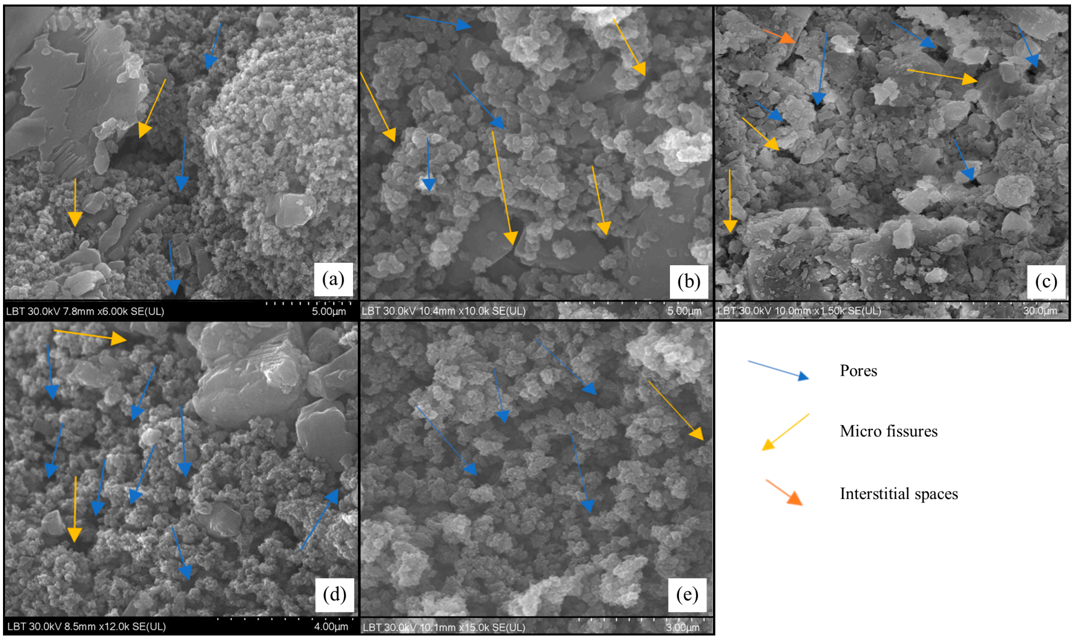

Figure 8. The SEM analyses performed on the rock fragments ((**a**)—2% nano-TiO_2 solution before introduction into CC; (**b**)—2% nano-TiO_2 solution after extraction from CC; (**c**)—reference sample after extraction from CC; (**d**)—5% nano-TiO_2 solution before introduction into CC; (**e**)—5% nano-TiO_2 solution, after extraction from CC).

Following the analysis of the SEM images of the samples coated with nano-TiO_2 before and after their exposure in CC, slight differences were highlighted within the ImageJ software. So, on average, the degree of coverage of the surfaces with nano-TiO_2 was 91.8% in the case of samples not introduced in the CC, and the degree of coverage decreased to 88.2% after exposure to the preset conditions within the CC. A loss of only 3.6% is minimal, which indicates that the nano-TiO_2 solution is very resistant to the weather and the action of boosted environmental factors (T and RH). In Figure 9, it can be seen that sample B3 lost only 3.66% coverage with nano-TiO_2 particles (from 90.16% initially to 87.50% after CC). The rock must be covered as much as possible with nano-TiO_2, but at the same time, it must not be completely covered to let the base surface breathe. This observation further underscores the efficacy and short-term durability of the nano-TiO_2 coating, highlighting its consistent performance under varying environmental conditions.

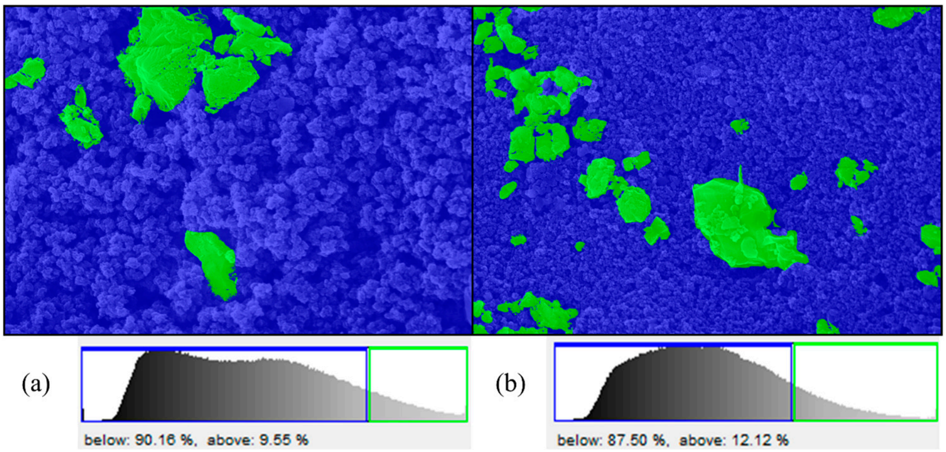

Figure 9. The results of the TiO_2—CA analysis indicating the degree of coverage of the rock with nano-TiO_2 nanoparticles before CC (**a**) and after exposure for six months in CC (**b**) (green color—base rock; blue color—nano-TiO_2 nanoparticles).

It is observed that from a crystallographic point of view, the dominant phase is represented by calcite with a trigonal crystal lattice, which is the most stable polymorphic form and is found in limestone rocks. The second identified crystallographic phase is silica, found in the form of quartz (Figure 10a). A comparison of the diffraction patterns upon the application of 2% nano-TiO_2 after the exposure in the CC is presented in Figure 10b. Nano-TiO_2 is found in the tetragonal polymorphic form of rutile, characterized by slightly broader diffraction peaks compared to calcite ones. Small quartz traces are also found in both patterns.

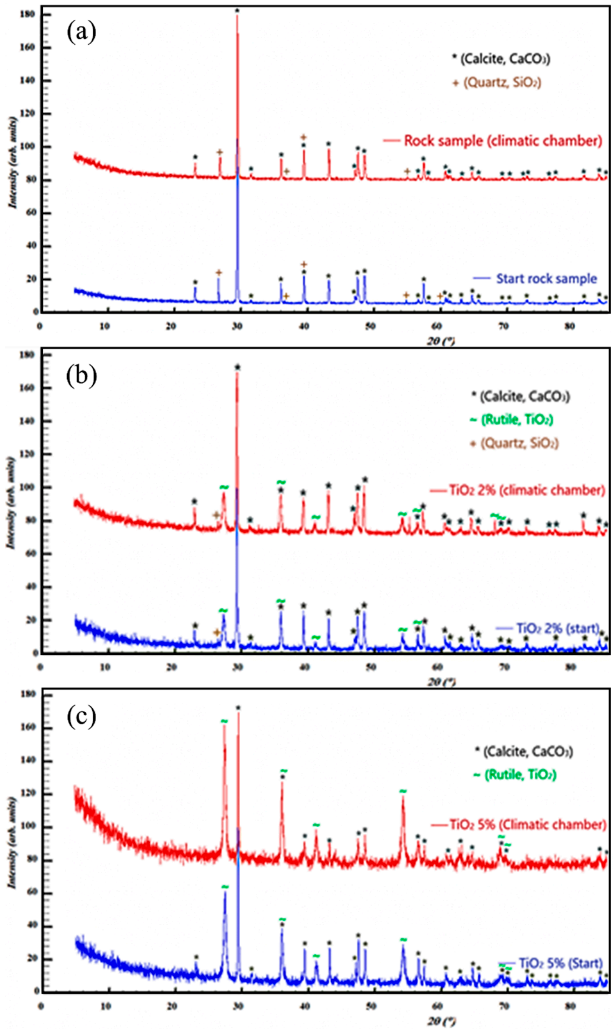

Figure 10. X-ray diffraction patterns of investigated samples ((**a**)—before exposure to CC; (**b**)—after exposure to CC—2% nano-TiO_2; (**c**)—after exposure to CC—5% nano-TiO_2).

The comparison of the diffraction patterns with a 5% nano-TiO_2 solution is presented in Figure 10c. With the increase in the concentration of the solution, a significant increase in the diffraction intensities specific to rutile is observed, and due to the consistency of the applied layer, the peaks corresponding to quartz disappear. In conclusion, with the exposure of the samples in CC with both 2% and 5% solutions, no structural changes are recorded; in other words, the nano-TiO_2 acts as a protective layer.

4. Conclusions

Nano-TiO_2 offers significant benefits for the preservation and protection of natural stone materials used for the façades of buildings and heritage objects located in the external or internal environment against climatic and environmental factors. Thus, regarding the morphological surfaces of the fossiliferous limestone surface, nano-TiO_2 tends to be distributed on the surface, filling the interior of micro-cracks, interstices, and pores, forming a protective layer that increases georesistance. The rock samples treated with nano-TiO_2 solutions (2% and 5%) showed a significantly higher compressive strength than the reference samples. The sample coated with 2% nano-TiO_2 showed a strength of 14.57 MPa, and the one coated with 5% nano-TiO_2 recorded 19.59 MPa. Comparatively, the reference samples showed values of approximately 9.55 MPa and 9.36 MPa, except for one sample that yielded 6.38 MPa. These results suggest that nano-TiO_2 can increase the mechanical strength of rocks, thus prolonging the life of construction materials, even in the case of a fossiliferous limestone like the one in the present study. Tests performed in the CC simulated extreme T and RH conditions similar to those that have the potential to occur in a UHI. The results showed that the nano-TiO_2 withstood these conditions well, maintaining their protective properties. Before and after exposure to the climatic conditions, the samples were analyzed using an electron microscope to assess the integrity of the nanoparticle layer. These analyses confirmed that the nano-TiO_2 remained well distributed and uniformly covered the rock surfaces, reducing micro-cracks and pores. The degree of nanoparticle surface coverage was 91.8% before CC exposure and slightly decreased to 88.2% after exposure to boosted climate conditions. This small loss indicates excellent weathering stability of the rock covered with nano-TiO_2.

The analysis of the samples with XRPD demonstrated that CC exposure did not change the composition of nano-TiO_2-treated rock, regardless of the concentration, whether 2% or 5%. These results confirm the chemical stability of the nano-TiO_2 treatment under varied climatic conditions, highlighting that both 2% and 5% concentrations maintain the mineralogical integrity of the rock without significant changes in composition.

The obtained results suggest that in the future, the management of natural stones for outdoor and indoor construction should include the usual expertise, including periodic visual inspections for the identification and monitoring of degradation and damage, up to more laborious analyses, in situ and ex situ, such as mineralogical–petrographic, RS analyses, diffractometry, and imaging. Also, the application of nanotechnology must be managed to evaluate and calibrate the objectives of preservation and conservation with the potential environmental and health risks (e.g., the emission of nano-TiO_2 particles into the air when applying the nano solution, as well as later in time). Their application can significantly reduce the need for frequent maintenance and help preserve the aesthetic appearance of heritage building façades. Although nano-TiO_2 offers multiple benefits for heritage conservation, it is important to manage its impact on the environment and human health. Inhalation of nanoparticles can pose risks, and their release into the environment must be monitored and controlled in situ.

5. Limitations and Future Works

Future research should explore optimized application methods to maximize these treatments' efficacy and durability. Long-term evaluation of the effectiveness of nano-TiO_2 is essential to ensure the chemical and aesthetic compatibility of these treatments with CH materials. Research should continue to explore new formulations and combinations of nanomaterials that can further improve the protection provided by nano-TiO_2. The use of nano-TiO_2 represents a promising solution for the conservation and protection of built CH, offering significant benefits in terms of compressive strength and durability in the face of climatic and environmental factors. However, careful application and long-term evaluation management is required to ensure these treatments' safety and efficacy.

In this study, the treatment with nano-TiO_2 was designed to form a protective layer on the surface of the fossiliferous limestone, which works by filling micro-cracks and reducing the porosity of the stone. This layer can limit the access of moisture and, implicitly, the transport of salt ions inside the material. Further testing may include exposing the treated samples to salt crystallization–dissolution cycles to determine to what extent the nano-TiO_2 can prevent or reduce the destructive effects of this phenomenon. This approach can provide a more complete understanding of the potential of these nanomaterials in the conservation of natural stone exposed to aggressive conditions. This is important for future applications, even if salt crystals were not observed in the analyses on the investigated samples.

The limitations of the present study include the analysis equipment with limited resolution and the experimental design, which did not allow a complete evaluation of the long-term effects of nano-TiO_2 on natural stone under real environmental conditions. At the same time, the fact that samples cannot be taken for better laboratory analyses due to the status of the building was an impediment.

Author Contributions: Conceptualization, D.C.I., A.-I.A., A.I. and T.C.; methodology, B.Z., A.T. and L.B.-T.; software, M.R. and E.-T.G.; validation, N.H. and T.H.H.; formal analysis, A.C.P., B.S. and B.B.; investigation, A.-I.A., D.C.I., B.Z. and B.S.; resources, T.H.H. and N.H.; data curation, T.C., A.I. and A.T.; writing—original draft preparation, D.C.I., A.I., T.C., A.C.P., B.B. and E.-T.G.; writing—review and editing, A.-I.A., B.Z., N.H. and A.T.; visualization, L.B.-T. and M.R.; supervision, D.C.I. All authors have read and agreed to the published version of the manuscript.

Funding: This work was supported by the Deanship of Scientific Research, Vice Presidency for Graduate Studies and Scientific Research, King Faisal University, Saudi Arabia [Grant No. KFU241658].

Data Availability Statement: The raw data supporting the conclusions of this article will be made available by the authors, without undue reservation.

Acknowledgments: The research undertaken was made possible by the equal scientific involvement of all the authors concerned. The research has been funded by the University of Oradea, Romania.

Conflicts of Interest: The authors declare no conflicts of interest.

Abbreviations

T	Temperatures
RH	Relative humidity
UHI	Urban heat island
RS	Raman Spectra
CT	Compression test
SEM	Scanning electron microscope
CC	Climatic chamber
XRPD	X-ray Powder Diffraction
CH	Cultural heritage
TiO_2	Titanium dioxide
TiO_2-CA	Titanium dioxide coverage analysis
nano-TiO_2	Titanium dioxide nanoparticles (<100 nm)

References

1. Li, H.; Wang, X.; Zhao, X.; Qi, Y. Understanding systemic risk induced by climate change. *Adv. Clim. Chang. Res.* **2021**, *12*, 384–394. [CrossRef]
2. Gburová, J.; Lukáč, M.; Matušíková, D. Impact of digital tools on the interest in visiting heritage objects in tourism. *GeoJ. Tour. Geosites* **2024**, *53*, 622–629. [CrossRef]
3. Pérez Gálvez, J.C.; Fuentes Jiménez, P.A.; Rodríguez Gutiérrez, P.; Medina Viruel, M.J. Emotional perception and cultural motivation on loyalty to a world heritage sites destination. *GeoJ. Tour. Geosites* **2023**, *49*, 1165–1175. [CrossRef]
4. Bogdan, A.; Chambre, D.; Copolovici, D.M.; Bungau, T.; Bungau, C.C.; Copolovici, L. Heritage Building Preservation in the Process of Sustainable Urban Development: The Case of Brasov Medieval City, Romania. *Sustain. Sci. Pract. Policy* **2022**, *14*, 6959. [CrossRef]
5. Sabbioni, C.; Cassar, M.; Brimblecombe, P.; Tidblad, J.; Kowslowski, R.; Drdácký, M.; Saint-Jimenez, C.; Grontoft, T.; Winewright, I.; Arino, X. Global Climate Change Impact on Built Heritage and Cultural Landscapes. In Proceedings of the International Conference on Heritage, Weathering and Conservation, HWC 2006, Spain, Madrid, 21–24 June 2006; de Buergo, F.A., Heraz, G., Calvo, V., Eds.; Tailor and Francis Group: London, UK, 2006; pp. 395–401.
6. Fatorić, S.; Daly, C. Towards a climate-smart cultural heritage management. *Wiley Interdiscip. Reviews. Clim. Chang.* **2023**, *14*, e855. [CrossRef]

7. Hedayatnia, H.; Steeman, M.; Van Den Bossche, N. Conservation of heritage buildings in Mashhad: On the impact of climate change and the urban heat island effect. In Proceedings of the 1st International Conference on Moisture in Buildings 2021 (ICMB21), Online, 28–29 June 2021. [CrossRef]
8. Zinzi, M.; Agnoli, S.; Burattini, C.; Mattoni, B. On the thermal response of buildings under the synergic effect of heat waves and urban heat island. *Sol. Energy* **2020**, *211*, 1270–1282. [CrossRef]
9. Guilbert, D.; Caluwaerts, S.; Calle, K.; Bossche, N.; Cnudde, V.; Kock, T. Impact of the urban heat island on freeze-thaw risk of natural stone in the built environment, a case study in Ghent, Belgium. *Sci. Total Environ.* **2019**, *677*, 9–18. [CrossRef]
10. Li, X.; Zhou, Y.; Yu, S.; Jia, G.; Li, H.; Li, W. Urban heat island impacts on building energy consumption: A review of approaches and findings. *Energy* **2019**, *174*, 407–419. [CrossRef]
11. Leal Filho, W.; Wolf, F.; Castro-Díaz, R.; Li, C.; Ojeh, V.N.; Gutiérrez, N.; Nagy, G.J.; Savić, S.; Natenzon, C.E.; Quasem Al-Amin, A.; et al. Addressing the Urban Heat Islands Effect: A Cross-Country Assessment of the Role of Green Infrastructure. *Sustain. Sci. Pract. Policy* **2021**, *13*, 753. [CrossRef]
12. Gomez-Villalba, L.S.; Salcines, C.; Fort, R. Application of Inorganic Nanomaterials in Cultural Heritage Conservation, Risk of Toxicity, and Preventive Measures. *Nanomaterials* **2023**, *13*, 1454. [CrossRef]
13. Ilies, D.C.; Blaga, L.; Ilies, A.; Pereș, A.C.; Caciora, T.; Hassan, T.H.; Hodor, N.; Turza, A.; Taghiyari, H.R.; Barbu-Tudoran, L.; et al. Green Biocidal Nanotechnology Use for Urban Stone-Built Heritage—Case Study from Oradea, Romania. *Minerals* **2023**, *13*, 1170. [CrossRef]
14. Ilieș, A.; Hodor, N.; Pantea, E.; Ilieș, D.C.; Indrie, L.; Zdrîncă, M.; Iancu, S.; Caciora, T.; Chiriac, A.; Ghergheles, C.; et al. Antibacterial Effect of Eco-Friendly Silver Nanoparticles and Traditional Techniques on Aged Heritage Textile, Investigated by Dark-Field Microscopy. *Coat. World* **2022**, *12*, 1688. [CrossRef]
15. Ilies, D.C.; Zlatev, Z.; Ilies, A.; Zharas, B.; Pantea, E.; Hodor, N.; Indrie, L.; Turza, A.; Taghiyari, H.R.; Caciora, T.; et al. Interdisciplinary Research to Advance Digital Imagery and Natural Compounds for Eco-Cleaning and for Preserving Textile Cultural Heritage. *Sensors* **2022**, *22*, 4442. [CrossRef] [PubMed]
16. Otero, J.; Borsoi, G.; Monasterio-Guillot, L. The Boom in Nanomaterials for Built Heritage Conservation: Why Does Size Matter? *Materials* **2023**, *16*, 3277. [CrossRef]
17. Munafò, P.; Goffredo, G.B.; Quagliarini, E. TiO_2-based nanocoatings for preserving architectural stone surfaces: An overview. *Constr. Build. Mater.* **2015**, *84*, 201–218. [CrossRef]
18. Ruffolo, S.A.; De Leo, F.; Ricca, M.; Arcudi, A.; Silvestri, C.; Bruno, L.; Urzì, C.; La Russa, M.F. Medium-term in situ experiment by using organic biocides and titanium dioxide for the mitigation of microbial colonization on stone surfaces. *Int. Biodeterior. Biodegrad.* **2017**, *123*, 17–26. [CrossRef]
19. Speziale, A.; González-Sánchez, J.F.; Taşcı, B.; Pastor, A.; Sánchez, L.; Fernández-Acevedo, C.; Oroz-Mateo, T.; Salazar, C.; Navarro-Blasco, I.; Fernández, J.M.; et al. Development of Multifunctional Coatings for Protecting Stones and Lime Mortars of the Architectural Heritage. *Int. J. Archit. Herit. Conserv. Anal. Restor.* **2020**, *14*, 1008–1029. [CrossRef]
20. Mirzaei, P. Recent challenges in modeling of urban heat island. *Sustain. Cities Soc.* **2015**, *19*, 200–206. [CrossRef]
21. Basu, S.; Orr, S.A.; Aktas, Y.D. A Geological Perspective on Climate Change and Building Stone Deterioration in London: Implications for Urban Stone-Built Heritage Research and Management. *Atmosphere* **2020**, *11*, 788. [CrossRef]
22. Buzgar, N.; Apopei, A.I. The Raman study of certain carbonates. *Geol. Tomul L* **2009**, *2*, 97–112.
23. Quagliarini, E.; Bondioli, F.; Goffredo, G.B.; Licciulli, A.; Munafò, P. Self-cleaning materials on Architectural Heritage: Compatibility of photo-induced hydrophilicity of TiO_2 coatings on stone surfaces. *J. Cult. Herit.* **2013**, *14*, 1–7. [CrossRef]
24. Sierra-Fernandez, A.; Gomez-Villalba, L.S.; Rabanal, M.E.; Fort, R. New nanomaterials for applications in conservation and restoration of stony materials: A review. *Mater. De Construcción* **2017**, *67*, e125. [CrossRef]
25. Xie, Z.; Duan, Z.; Zhao, Z.; Li, R.; Zhou, B.; Yang, D.; Hu, Y. Nano-materials enhanced protectants for natural stone surfaces. *Herit. Sci.* **2021**, *9*, 122. [CrossRef]
26. Chen, X.; Mao, S.S. Titanium dioxide nanomaterials: Synthesis, properties, modifications, and applications. *Chem. Rev.* **2012**, *107*, 2891–2959. [CrossRef] [PubMed]
27. Linkous, C.; Carter, G.; Locuson, D.; Ouellette, A.; Slattery, D.; Smitha, L. Photocatalytic Inhibition of Algae Growth Using TiO_2, WO_3, and Cocatalyst Modifications. *Environ. Sci. Technol.* **2000**, *34*, 4754–4758. [CrossRef]
28. Aldoasri, M.; Darwish, S.; Adam, M.; Elmarzugi, N.; Ahmed, S. Protecting Marble Stone Facades of Historic Buildings Using Multifunctional TiO_2 Nanocoatings. *Sustainability* **2017**, *9*, 2002. [CrossRef]
29. Colangiuli, D.; Lettieri, M.; Masieri, M.; Calia, A. Field study in an urban environment of simultaneous self-cleaning and hydrophobic nanosized TiO_2-based coatings on stone for the protection of building surface. *Sci. Total Environ.* **2019**, *650 Pt 2*, 2919–2930. [CrossRef]
30. Pozo-Antonio, J.S.; Noya, D.; Montojo, C. Aesthetic Effects on Granite of Adding Nanoparticle TiO_2 to Si-Based Consolidants (Ethyl Silicate or Nano-Sized Silica). *Coatings* **2020**, *10*, 215. [CrossRef]
31. Calia, A.; Lettieri, M.; Masieri, M. Durability assessment of nanostructured TiO_2 coatings applied on limestones to enhance building surface with self-cleaning ability. *Build. Environ.* **2016**, *110*, 1–10. [CrossRef]
32. Veltri, S.; Palermo, A.M.; De Filpo, G.; Xu, F. Subsurface treatment of TiO_2 nanoparticles for limestone: Prolonged surface photocatalytic biocidal activities. *Build. Environ.* **2019**, *149*, 655–661. [CrossRef]

33. Kanth, A.P.; Soni, A.K. Application of Nanocomposites for Conservation of Materials of Cultural Heritage. *J. Cult. Herit.* **2023**, *59*, 120–130. [CrossRef]
34. La Russa, M.F.; Rovella, N.; Alvarez de Buergo, M.; Belfiore, C.M.; Pezzino, A.; Crisci, G.M.; Ruffolo, S.A. Nano-TiO_2 coatings for cultural heritage protection: The role of the binder on hydrophobic and self-cleaning efficacy. *Prog. Org. Coat.* **2015**, *89*, 16–25. [CrossRef]
35. Gherardi, F.; Colombo, A.; Goidanich, S.; Toniolo, L. *Smart Hydrophobic TiO_2 Nanocomposites for the Protection of Stone Cultural Heritage*; Paisley University of the West of Scotland: Paisley, UK, 2016; pp. 325–332.
36. Battistel, E.; Favaro, M.; Tomasin, P.; Gambirasi, A. Photocatalytic TiO_2-based nanocoating for the preservation of historical limestone buildings. *J. Cult. Herit.* **2017**, *23*, 120–128.
37. Ionescu, A.; Popescu, B.; Marin, C.; Dumitrescu, D.; Georgescu, E.; Vasilescu, F. Efectele tratamentului cu TiO_2 pe fațadele monumentelor medievale din piatră. *Rev. De Conserv. A Patrim. Cult.* **2021**, *8*, 67–78.
38. Popovici, C.; Stanciu, M.; Ionescu, R.; Mihai, L.; Dumitru, A.; Stoica, S. Impactul aplicării TiO_2 pe mobilierul istoric din lemn. *Rev. De Conserv. Și Restaur.* **2022**, *11*, 78–89.
39. Baglioni, P.; Carretti, E.; Dei, L. Colloid and materials science for the conservation of cultural heritage: Cleaning, consolidation, and deacidification. *Langmuir* **2014**, *30*, 2691–2703. [CrossRef] [PubMed]
40. Ben Chobba, M.; Weththimuni, M.L.; Messaoud, M.; Urzi, C.; Licchelli, M. Recent Advances in the Application of Metal Oxide Nanomaterials for the Conservation of Stone Artefacts, Ecotoxicological Impact and Preventive Measures. *Coat. World* **2024**, *14*, 203. [CrossRef]
41. Goffredo, G.B.; Munafò, P. Preservation of Historical Stone Surfaces by TiO_2 Nanocoatings. *Coat. World* **2015**, *5*, 222–231. [CrossRef]
42. Rodriguez, C.; Martinez, A.; Lopez, J.; Hernandez, P.; Sanchez, R.; Gomez, M.; Fernandez, E. Physical and Chemical Modifications Induced by TiO_2 Coatings on Stone Materials: A Critical Review. *J. Mater. Eng.* **2020**, *25*, 210–225.
43. Smith, D.; Johnson, L.; Brown, T.; Williams, R.; Lee, S.; Thompson, K. Recent Developments in TiO_2 Application for Stone Conservation: A Review. *J. Cult. Herit. Preserv.* **2021**, *18*, 45–60.
44. Costanzo, A.; Ebolese, D.; Ruffolo, S.A.; Falcone, S.; la Piana, C.; La Russa, M.F.; Musacchio, M.; Buongiorno, M.F. Detection of the TiO_2 Concentration in the Protective Coatings for the Cultural Heritage by Means of Hyperspectral Data. *Sustainability* **2021**, *13*, 92. [CrossRef]
45. Pinna, D.; Salvadori, B.; Galeotti, M. Monitoring the performance of innovative nanoparticles for the conservation of historical stones. *J. Cult. Herit.* **2013**, *14*, 15–21.
46. Smith, J.; Davis, H.; Miller, P.; Clark, A.; Wilson, E.; Roberts, M. The Aesthetic Effects of TiO_2 Application on Stone Surfaces: A Review. *J. Aesthet. Conserv.* **2017**, *14*, 78–89.
47. Liu, Y.; Chen, X.; Wang, Z.; Zhang, L.; Yang, F.; Zhao, Q. Investigating the Impact of TiO_2 Coatings on Stone Surface Aesthetics: A Comparative Study. *J. Stone Mater. Aesthet.* **2020**, *18*, 112–125.
48. Keller, A.A.; McFerran, S.; Lazareva, A.; Suh, S. Global life cycle releases of engineered nanomaterials. *J. Nanoparticle Res.* **2013**, *15*, 1692. [CrossRef]
49. Li, M.; Zhou, Y.; Wang, H.; Xu, J.; Zhang, D.; Chen, L.; Sun, J. Health Implications of TiO_2 Nanoparticle Exposure: A Review. *J. Nanotoxicology* **2012**, *16*, 112–125.
50. Cho, Y.; Kim, S.; Park, J.; Lee, H.; Choi, K.; Lim, D.; Shin, J. Assessing the Health Effects of TiO_2 Nanoparticles: Current Understanding and Future Directions. *J. Health Sci.* **2018**, *25*, 210–223.
51. Zifceac, I.; Paunescu, C.; Vais, M. The Impact of the Green Spaces On the Land Surface Temperature in Urban Areas—Analysis of the Land Surface Temperature in the City of Oradea using Landsat 8 Satellite Images. Bulletin of the Transilvania University of Brasov. *Ser. I—Eng. Sci.* **2022**, *15*, 55–62. [CrossRef]
52. Pașca, M. *Arhitectul Frigyes Spiegel la Oradea*; Editura Arca Oradea: Oradea, Romania, 2010; ISBN 978-973-1881-49-2.
53. Pașca, M. *Oradea 1900: Un Ghid de Arhitectură*, 3rd ed.; Editura Argonaut: Cluj-Napoca, Rumania, 2019; ISBN 978-973-109-932-3.
54. Croitoru, A.-E.; Holobaca, I.-H.; Lazar, C.; Moldovan, F.; Imbroane, A. Air temperature trend and its impact on winter wheat phenology in Romania. *Clim. Chang.* **2012**, *111*, 393–410. [CrossRef]
55. Herbel, I.; Croitoru, A.-E.; Rus, I.; Harpa, G.V.; Ciupertea, A.F. Detection of atmospheric urban heat island through direct measurements in Cluj-Napoca city, Romania. *Hung. Geogr. Bull.* **2016**, *65*, 117–128. [CrossRef]
56. Lloyd, G.; Farmer, A.; Mainprice, D. Misorientation analysis and the formation and orientation of subgrain and grain boundaries. *Tectonophysics* **1997**, *279*, 55–78. [CrossRef]
57. Foucher, F.; Guimbretière, G.; Bost, N.; Westall, F. Petrographical and mineralogical applications of Raman mapping. In *Raman Spectroscopy and Applications*; InTech: Penang, Malaysia, 2017. [CrossRef]
58. Búrdalo-Salcedo, G.; Rodríguez, I.; Fernández-Raga, M.; Fernández-Raga, S.; Rodríguez-Fernández, C.; González-Domínguez, J.M. Adaptation of a Standard Method for Water Absorption Testing of Stone Materials: The Case of a Hydrophilic Protective Coating. *Materials* **2023**, *16*, 4228. [CrossRef] [PubMed]
59. Otero, J.; Pozo-Antonio, J.S.; Montojo, C. Influence of application method and number of applications of nanolime on the effectiveness of the Doulting limestone treatments. *Mater. Struct.* **2021**, *54*, 41. [CrossRef]
60. *UNE EN 1926:2007*; Natural Stone Test Methods—Determination of Uniaxial Compressive Strength. AENOR: Madrid, Spain, 2007.

61. Banc, S.; Croitoru, A.-E.; David, N.A.; Scripcă, A.-S. Changes Detected in Five Bioclimatic Indices in Large Romanian Cities over the Period 1961–2016. *Atmosphere* **2020**, *11*, 819. [CrossRef]
62. Lawrence, M. The relationship between relative humidity and the dewpoint temperature in moist air—A simple conversion and applications. *Bull. Am. Meteorol. Soc.* **2005**, *86*, 225–233. [CrossRef]
63. Butler, B.M.; Hillier, S. powdR: An R package for quantitative mineralogy using full pattern summation of X-ray powder diffraction data. *Comput. Geosci.* **2021**, *147*, 104662. [CrossRef]
64. Martínez-García, R.; González-Campelo, D.; Fraile-Fernández, F.J.; Castañón, A.M.; Caldevilla, P.; Giganto, S.; Ortiz-Marqués, A.; Zelli, F.; Calvo, V.; González-Domínguez, J.M.; et al. Performance study of graphene oxide as an antierosion coating for ornamental and heritage dolostone. *Adv. Mater. Technol.* **2023**, *8*, 2300486. [CrossRef]
65. Dorobat, M.L.; Balta, M.M.; Dobrescu, C.M. Comparative study of some geomechanical properties of the limestones and shists in the screes of Leaota Massif (Southern Carpathians, Romania). *Curr. Trends Nat. Sci.* **2018**, *7*, 12–21.
66. Lazzari, M.; Bianchi, S.; Rossi, F.; Conti, G.; Romano, L.; Greco, P. Enhancing Stone Surface Resistance to Environmental Stress Factors with TiO_2 Nanoparticles. *J. Stone Mater. Sci.* **2018**, *12*, 45–58.